



HAL
open science

Erosion of the chronic myeloid leukaemia stem cell pool by PPAR γ agonists

Stéphane Prost, Francis Relouzat, Marc Spentchian, Yasmine Ouzegdouh,
Joseph Saliba, Gérald Massonnet, Jean-Paul Beressi, Els Verhoeyen, Victoria
Raggueneau, Benjamin Maneglier, et al.

► **To cite this version:**

Stéphane Prost, Francis Relouzat, Marc Spentchian, Yasmine Ouzegdouh, Joseph Saliba, et al.. Erosion of the chronic myeloid leukaemia stem cell pool by PPAR γ agonists. *Nature*, 2015, 525 (7569), pp.380-383. 10.1038/nature15248 . hal-01911062

HAL Id: hal-01911062

<https://hal.science/hal-01911062>

Submitted on 27 Aug 2020

HAL is a multi-disciplinary open access archive for the deposit and dissemination of scientific research documents, whether they are published or not. The documents may come from teaching and research institutions in France or abroad, or from public or private research centers.

L'archive ouverte pluridisciplinaire **HAL**, est destinée au dépôt et à la diffusion de documents scientifiques de niveau recherche, publiés ou non, émanant des établissements d'enseignement et de recherche français ou étrangers, des laboratoires publics ou privés.

Erosion of the chronic myeloid leukaemia stem cell pool by PPAR γ agonists

Stéphane Prost¹, Francis Relouzat¹, Marc Spentchian², Yasmine Ouzegdouh¹, Joseph Saliba¹, Gérald Massonnet³, Jean-Paul Beressi⁴, Els Verhoeyen^{5,6}, Victoria Raggiueneau⁷, Benjamin Maneglier⁸, Sylvie Castaigne⁹, Christine Chomienne³, Stany Chrétien^{1,10*}, Philippe Rousselot^{3,9*} & Philippe Leboulch^{1,11,12*}

Whether cancer is maintained by a small number of stem cells or is composed of proliferating cells with approximate phenotypic equivalency is a central question in cancer biology¹. In the stem cell hypothesis, relapse after treatment may occur by failure to eradicate cancer stem cells. Chronic myeloid leukaemia (CML) is quintessential to this hypothesis. CML is a myeloproliferative disorder that results from dysregulated tyrosine kinase activity of the fusion oncoprotein BCR-ABL². During the chronic phase, this sole genetic abnormality (chromosomal translocation Ph⁺: t(9;22)(q34;q11)) at the stem cell level causes increased proliferation of myeloid cells without loss of their capacity to differentiate. Without treatment, most patients progress to the blast phase when additional oncogenic mutations result in a fatal acute leukaemia made of proliferating immature cells. Imatinib mesylate and other tyrosine kinase inhibitors (TKIs) that target the kinase activity of BCR-ABL have improved patient survival markedly. However, fewer than 10% of patients reach the stage of complete molecular response (CMR), defined as the point when BCR-ABL transcripts become undetectable in blood cells³. Failure to reach CMR results from the inability of TKIs to eradicate quiescent CML leukaemia stem cells (LSCs)²⁻⁴. Here we show that the residual CML LSC pool can be gradually purged by the glitazones, antidiabetic drugs that are agonists of peroxisome proliferator-activated receptor- γ (PPAR γ). We found that activation of PPAR γ by the glitazones decreases expression of STAT5 and its downstream targets HIF2 α ⁵ and CITED2⁶, which are key guardians of the quiescence and stemness of CML LSCs. When pioglitazone was given temporarily to three CML patients in chronic residual disease in spite of continuous treatment with imatinib, all of them achieved sustained CMR, up to 4.7 years after withdrawal of pioglitazone. This suggests that clinically relevant cancer eradication may become a generally attainable goal by combination therapy that erodes the cancer stem cell pool.

Cell division tracking with carboxyfluorescein diacetate-succinimidyl ester (CFSE) indicates that non-cycling CML cells are poorly sensitive to TKIs^{7,8} and that the quiescent TKI-resistant subpopulation is enriched in CD34⁺CD38⁻ cells⁹. CML LSCs are hence similar to normal quiescent haematopoietic stem cells (HSCs), although they are cytokine-independent⁷. Because failure to reach CMR occurs even when BCR-ABL remains sensitive to TKIs², we searched for possible 'non-oncogene addiction (NOA)' of CML LSCs as a novel therapeutic target. NOA indicates that a given malignant cell is abnormally sensitive to quantitative variations in an otherwise normal molecular pathway¹⁰.

We previously reported that the Nef proteins of the immunodeficiency viruses impair haematopoiesis by activating peroxisome

proliferator-activated receptor gamma (PPAR γ)¹¹. This effect was reproduced by the thiazolidinediones, a class of synthetic PPAR γ ligands (Extended Data Fig. 1a), although it is compensated in individuals with otherwise normal haematopoiesis¹². We then became intrigued with our observation that the CML cell line K562 is particularly sensitive to Nef and thiazolidinediones¹¹. The involvement of PPAR γ was also more recently reported in haematopoietic stress response¹³.

We turned to a cohort of 29 chronic phase (CP) CML patients at diagnosis whose CD34⁺ cells were >95% Ph⁺. Combining imatinib and pioglitazone showed evidence of synergy with a decrease in the number of colony-forming cells (CFC) sixfold more pronounced ($P < 0.0001$) than with imatinib alone (Extended Data Fig. 2a). A similar trend was observed when normal CD34⁺ cells were transduced with a lentiviral vector expressing p210 BCR-ABL (Extended Data Fig. 2b). Whereas imatinib alone was unable to reduce significantly the frequency of CP-CML long term culture-initiating cells (LTC-ICs) ($P = 0.067$), we found that pioglitazone was able to do so, either as a single agent by 2.4-fold ($P = 0.008$) or with an improved effect by 3.5-fold in the presence of imatinib ($P < 0.001$) (Fig. 1a, b). Similar results were obtained with the second generation TKI dasatinib or with another thiazolidinedione, rosiglitazone (Extended Data Fig. 2c, d).

CFSE assays were then performed with CP-CML CD34⁺ cells in the absence of cytokines (Fig. 1c-e and Extended Data Table 1). Untreated control CP-CML CD34⁺ cells proliferated and differentiated actively. Imatinib exposure resulted in the elimination of actively dividing cells but also in the accumulation of viable CFSE-bright CD34⁺ cells that never divided ('P') or had divided only once (Fig. 1d). Pioglitazone alone was less effective than imatinib to deplete the bulk of dividing CML cells but triggered exit from quiescence (Fig. 1c-e and Extended Data Table 1). Combining pioglitazone with either imatinib or dasatinib acted in synergy to deplete both proliferating and non-proliferating cells (Fig. 1c-e, Extended Data Table 1 and Extended Data Fig. 2e). Imatinib alone was effective at decreasing the number of Ph⁺ CD34⁺ CD38⁺ progenitors but failed to reduce the more immature CD34⁺ CD38⁻ population, opposite to pioglitazone alone (Extended Data Fig. 3b).

We then investigated the possible molecular pathways that mediate pioglitazone activity against CML LSCs. We previously reported that PPAR γ is a negative transcriptional regulator of STAT5 (A and B)¹¹. STAT5 is known to be critical for maintenance and fitness of both normal HSCs¹⁴ and CML cells, where STAT5 is activated upon direct phosphorylation by the BCR-ABL kinase¹⁵. STAT5 expression levels were abnormally high in both total CP-CML CD34⁺ cells and quiescent LSC (Fig. 2a). In CFSE-bright cells (that is, P and 1 division of

¹CEA, Institute of Emerging Diseases and Innovative Therapies (IMETI), F-92265 Fontenay-aux-Roses, France. ²Département de biologie médicale, Hôpital Mignot, F-78150 Le Chesnay, France. ³Unité de Biologie Cellulaire, UMR-S-940 Institut Universitaire d'Hématologie, Hôpital Saint Louis, F-75010 Paris, France. ⁴Service d'Endocrinologie et de Diabétologie, Hôpital Mignot, F-78150 Le Chesnay, France. ⁵CIRI, International Center for Infectiology Research, EVIR team, Inserm, U1111, CNRS, UMR5308, Université de Lyon-1, ENS de Lyon, 69007 Lyon, France. ⁶Inserm, U895, Centre de Médecine Moléculaire (C3M), équipe 3, 06204 Nice, France. ⁷Laboratoire d'hématologie, Centre Hospitalier de Versailles, F-78150 Le Chesnay, France. ⁸Unité de Pharmacologie, Service de Biologie Médicale, Centre Hospitalier de Versailles, F-78150 Le Chesnay, France. ⁹Service d'Hématologie et d'Oncologie, Hôpital Mignot, Université Versailles Saint-Quentin-en-Yvelines, F-78150 Le Chesnay, France. ¹⁰Inserm, Institute of Emerging Diseases and Innovative Therapies (IMETI), F-92265 Fontenay-aux-Roses, France. ¹¹Genetics Division, Brigham & Women's Hospital and Harvard Medical School, Boston, Massachusetts 02115, USA. ¹²Hematology Division, Ramathibodi Hospital and Mahidol University, 10400 Bangkok, Thailand.

*These authors contributed equally to this work.

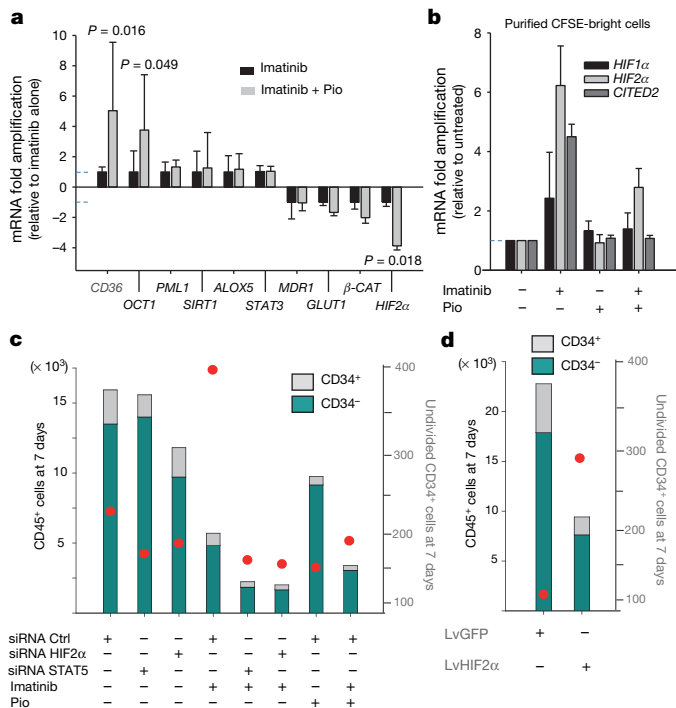


Figure 3 | Expression of target genes in CP-CML cells exposed to pioglitazone and imatinib. **a**, RT-qPCR assays on CP-CML CD34⁺ cells after 7 days without serum or cytokines. Data show means + s.d., $n = 11$. **b**, RT-qPCR assays in purified 12–14 days CFSE-bright cells (that is, P and 1 division). Data show means + s.d., $n = 6$. **c**, Absolute cell count together with CFSE analysis of representative CP-CML patient 8 (triplicate). Undivided cells (red dots). Also see Extended Data Fig. 7 and Extended Data Fig. 1c. **d**, Same as in **c**, but after transduction of cord blood CD34⁺ cells with lentivectors (Lv) (triplicate). Undivided cells (red dots). See statistics in Methods.

Data Fig. 8a, b). Because *CITED2* is a known master gene of HSC quiescence that regulates stemness-associated genes such as *BMI1*²², *HES1*²³ and *p57* (also known as *CDKN1C*)²³, we studied the expression of these genes in CD34⁺ cells from CP-CML patients and in murine Ba/F3 cell lines we generated to express, by means of retroviral vector transduction and ubiquitous promoter driven expression, the constitutively active forms of murine Stat5a or Stat5b 1*6 (H299R, S711F). After 10 days of culture in the presence of imatinib, TKI-resistant CD34⁺ cells from CP-CML patients showed an increase in endogenous expression of both *CITED2* itself (4.5-fold) and the known *CITED2* target genes *BMI1* (2.8-fold), *HES1* (3.1-fold) and *p57* (16.5-fold). Addition of pioglitazone fully counteracted said increase in *CITED2*, *BMI1* and *HES1* expression and reduced the increase in *p57* expression by fourfold (Extended Data Fig. 9a). Ba/F3 cell studies corroborated this evidence (Extended Data Fig. 9b and c). Taken together, we propose here that the CML-LSC is critically dependent (NOA) on a PPAR γ -STAT5-HIF2 α -CITED2 pathway, directly and effectively inhibited by pioglitazone (Fig. 4a), thus extending the contention that equivalent murine leukaemias are addicted (NOA) to STAT5 (ref. 15).

Because mouse models are poorly suited to investigate CML LSCs²⁴ and pioglitazone is an approved drug for the treatment of diabetes mellitus type 2 in humans, we initially sought to validate pioglitazone directly on two patients diagnosed with both diabetes and CML who never reached CMR in spite of long-term imatinib treatment. Before filing a formal clinical trial application, we prescribed pioglitazone off-label and under approved informed consent to a third CML patient, this time non-diabetic, who never reached CMR either under long-term imatinib therapy (Fig. 4b).

Pioglitazone was added to the treatment after 5, 6 and 4 years of uninterrupted imatinib therapy for patients 1, 2 and 3, respectively. None of the 3 patients ever reached CMR before introduction of

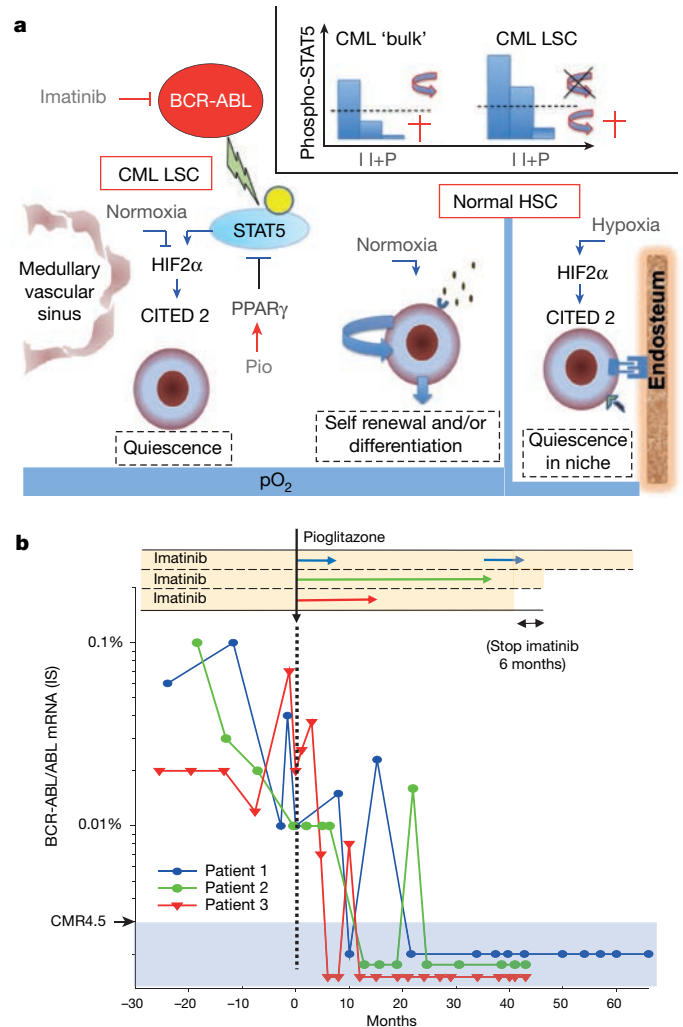


Figure 4 | Pioglitazone induces complete and sustained molecular response (CMR) in CML patients. **a**, Model of CML LSC addiction to the PPAR γ -STAT5-HIF2 α pathway. (Top insert) for the bulk of dividing CML cells, imatinib (I) alone is able to bring phospho-STAT5 levels below a threshold (dotted line) at which apoptosis occurs (cross). For CML LSCs, only the combination of imatinib and pioglitazone (I+P) is able to bring cells below a threshold at which cells leave their state of quiescence before undergoing apoptosis. **b**, RT-qPCR assays for *BCR-ABL/ABL* on nucleated blood cells from the first three patients. See Supplementary Information for details.

pioglitazone. Pioglitazone was added to the treatment of patient 1 during two brief exposures of 10 and 8 months each with an interval of 28 months (Fig. 4b). CMR was achieved 10 months after initial pioglitazone addition, and patient 1 has remained in CMR for at least 56 months, the last time-point collected for this study, which is 53 months (4.5 years) after first stopping pioglitazone administration (Fig. 4b). For patient 2, CMR was obtained after 1 year of pioglitazone addition and maintained for 32 months at which time they withdrew (Fig. 4b). For patient 3, CMR was achieved after 6 months of pioglitazone addition. At this time point, the level of *STAT5* mRNA in CD34⁺ cells from the bone marrow of patient 3 was decreased by 11.9 fold. Patient 3 has remained in CMR for at least 38 months, the last time-point collected for this study, which is 28 months after stopping pioglitazone administration (Fig. 4b). Furthermore, patient 3 decided to stop imatinib for the last 6 months of the aforementioned observation period and has remained in CMR during this period without any treatment (Fig. 4b and Supplementary Data).

Regulatory approval was then obtained for multi-centre Phase II clinical trials, and the first (EudraCT 2009-011675-79) aimed at assessing the short-term cumulative incidence of CMR conversion

for patients who never reached CMR under imatinib alone (<https://www.clinicaltrialsregister.eu/ctr-search/trial/2009-011675-79/FR#E>). Scoring by quantitative PCR was performed over the course of the first 12 months after trial initiation during concurrent and brief exposure (3 to 12 months) to the imatinib-pioglitazone combination²⁵. Out of 24 assessable patients, the cumulative incidence rate in the treated group reached 57% versus 27% ($P = 0.02$) for an historical group of patients having received imatinib alone, thus indicating that clinical evidence of efficacy can already be detected even after very brief treatment and early analysis. Post-trial follow-up confirmed stability of CMR status in data collected to date. Therapy with pioglitazone was accompanied by a stable reduction of *STAT5* mRNA in patient samples as early as month 6 (2.3-fold, $P = 0.0003$) and by a reduction of the clonogenic potential of bone marrow CD34⁺ cells (1.54-fold, $P = 0.0003$).

Although both imatinib and pioglitazone decrease *STAT5* activity, they act by different mechanisms. Imatinib inhibits *STAT5* activation by BCR-ABL phosphorylation, whereas pioglitazone decreases *STAT5* expression. It seems that imatinib alone is sufficient to induce effective clearance of the bulk of more differentiated CML cells, but fails to bring *STAT5* activity below a threshold for CML LSC to exit from quiescence and to undergo subsequent apoptosis. Pioglitazone is effective at doing so in synergy with imatinib (Fig. 4a, top insert). As in this example with CML, progressive erosion of cancer stem cell pools may prove ultimately achievable pharmacologically, bringing hope of obtaining cancer eradication in a variety of human malignancies by combination therapy.

Online Content Methods, along with any additional Extended Data display items and Source Data, are available in the online version of the paper; references unique to these sections appear only in the online paper.

Received 17 March 2014; accepted 28 July 2015.

Published online 2 September 2015.

- Nguyen, L. V., Vanner, R., Dirks, P. & Eaves, C. J. Cancer stem cells: an evolving concept. *Nature Rev. Cancer* **12**, 133–143 (2012).
- Chomel, J. C. & Turhan, A. G. Chronic myeloid leukemia stem cells in the era of targeted therapies: resistance, persistence and long-term dormancy. *Oncotarget* **2**, 713–727 (2011).
- de Lavallade, H. *et al.* Imatinib for newly diagnosed patients with chronic myeloid leukemia: incidence of sustained responses in an intention-to-treat analysis. *J. Clin. Oncol.* **26**, 3358–3363 (2008).
- Corbin, A. S. *et al.* Human chronic myeloid leukemia stem cells are insensitive to imatinib despite inhibition of BCR-ABL activity. *J. Clin. Invest.* **121**, 396–409 (2011).
- Hu, C. J., Sataur, A., Wang, L., Chen, H. & Simon, M. C. The N-terminal transactivation domain confers target gene specificity of hypoxia-inducible factors HIF-1 α and HIF-2 α . *Mol. Biol. Cell* **18**, 4528–4542 (2007).
- Du, J. & Yang, Y. C. Cited2 in hematopoietic stem cell function. *Curr. Opin. Hematol.* **20**, 301–307 (2013).
- Graham, S. M. *et al.* Primitive, quiescent, Philadelphia-positive stem cells from patients with chronic myeloid leukemia are insensitive to ST1571 *in vitro*. *Blood* **99**, 319–325 (2002).
- Jørgensen, H. G., Allan, E. K., Jordanides, N. E., Mountford, J. C. & Holyoake, T. L. Nilotinib exerts equipotent antiproliferative effects to imatinib and does not induce apoptosis in CD34⁺ CML cells. *Blood* **109**, 4016–4019 (2007).
- Copland, M. *et al.* Dasatinib (BMS-354825) targets an earlier progenitor population than imatinib in primary CML but does not eliminate the quiescent fraction. *Blood* **107**, 4532–4539 (2006).
- Luo, J., Solimini, N. L. & Elledge, S. J. Principles of cancer therapy: oncogene and non-oncogene addiction. *Cell* **136**, 823–837 (2009).
- Prost, S. *et al.* Human and simian immunodeficiency viruses deregulate early hematopoiesis through a Nef/PPAR γ /STAT5 signaling pathway in macaques. *J. Clin. Invest.* **118**, 1765–1775 (2008).
- Berria, R. *et al.* Reduction in hematocrit and hemoglobin following pioglitazone treatment is not hemodilutional in Type II diabetes mellitus. *Clin. Pharmacol. Ther.* **82**, 275–281 (2007).
- Avagyan, S., Aguilo, F., Kamezaki, K. & Snoeck, H. W. Quantitative trait mapping reveals a regulatory axis involving peroxisome proliferator-activated receptors, PRDM16, transforming growth factor- β 2 and FLT3 in hematopoiesis. *Blood* **118**, 6078–6086 (2011).
- Wang, Z., Li, G., Tse, W. & Bunting, K. D. Conditional deletion of *STAT5* in adult mouse hematopoietic stem cells causes loss of quiescence and permits efficient nonablative stem cell replacement. *Blood* **113**, 4856–4865 (2009).
- Hoelbl, A. *et al.* *Stat5* is indispensable for the maintenance of *bcr/abl*-positive leukaemia. *EMBO Mol. Med.* **2**, 98–110 (2010).
- Kieslinger, M. *et al.* Antiapoptotic activity of *Stat5* required during terminal stages of myeloid differentiation. *Genes Dev.* **14**, 232–244 (2000).
- Fatrai, S., Wierenga, A. T., Daenen, S. M., Vellenga, E. & Schuringa, J. J. Identification of *HIF2 α* as an important *STAT5* target gene in human hematopoietic stem cells. *Blood* **117**, 3320–3330 (2011).
- Matsumoto, A. *et al.* CIS, a cytokine inducible SH2 protein, is a target of the JAK-*STAT5* pathway and modulates *STAT5* activation. *Blood* **89**, 3148–3154 (1997).
- Liu, S. *et al.* Targeting *STAT5* in hematologic malignancies through inhibition of the bromodomain and extra-terminal (BET) bromodomain protein BRD2. *Mol. Cancer Ther.* **13**, 1194–1205 (2014).
- Wang, L., Giannoudis, A., Austin, G. & Clark, R. E. Peroxisome proliferator-activated receptor activation increases imatinib uptake and killing of chronic myeloid leukemia cells. *Exp. Hematol.* **40**, 811–819 (2012).
- Szanto, A. & Nagy, L. Retinoids potentiate peroxisome proliferator-activated receptor gamma action in differentiation, gene expression, and lipid metabolic processes in developing myeloid cells. *Mol. Pharmacol.* **67**, 1935–1943 (2005).
- Chen, Y., Haviernik, P., Bunting, K. D. & Yang, Y. C. Cited2 is required for normal hematopoiesis in the murine fetal liver. *Blood* **110**, 2889–2898 (2007).
- Du, J. *et al.* HIF-1 α deletion partially rescues defects of hematopoietic stem cell quiescence caused by Cited2 deficiency. *Blood* **119**, 2789–2798 (2012).
- Koschmieder, S. & Schemionek, M. Mouse models as tools to understand and study BCR-ABL1 diseases. *Am. J. Blood Res.* **1**, 65–75 (2011).
- Rousselot, P. *et al.* Targeting *STAT5* expression resulted in molecular response improvement in patients with chronic phase CML treated with imatinib. *ASH Annual Meeting Abstracts*, (2012).

Supplementary Information is available in the online version of the paper.

Acknowledgements We thank C. Costa, V. Tran Chau, F. Goullieux, A. Krief, P. Raynal, C. Terré, S. Taboré and T. Andrieu for their experimental contributions. This work was supported by the Association Laurette Fugain, Paris, France, by the Association pour la Recherche sur le Cancer, Villejuif, France to S.P., P.R. and P.L. and by the Chaire industrielle de l'Agence Nationale pour la Recherche (ANR) to P.L.

Author Contributions S.P. lead the project, designed and performed experiments, and analysed data. P.L. and S.Ch. designed experiments and analysed data. P.L. wrote the paper. F.R., M.S., Y.O., J.S., E.V., V.R., B.M. and G.M. contributed experimentally. P.R., J.-P.B., C.C. and S.Ca. contributed clinically. P.R., S.Ch. and P.L. have contributed equally to this work; P.R. in a clinical capacity, S.C. and P.L. in a scientific capacity.

Author Information Reprints and permissions information is available at www.nature.com/reprints. The authors declare no competing financial interests. Readers are welcome to comment on the online version of the paper. Correspondence and requests for materials should be addressed to S.P. (stephane.prost@cea.fr) and P.L. (pleboulch@rics.bwh.harvard.edu).

METHODS

Reagents. For *in vitro* assays, PPAR γ agonists were provided by Cayman Chemical (PPAR γ -PAK; Bertin-pharma). Imatinib mesylate was provided by Novartis and was used at 1 μ M in culture, a well-established inhibitory concentration *in vitro* that also approaches the achievable drug level in patients' plasma. Dasatinib and JQ1 were provided by Bristol-Myers Squibb and Sigma and were used in culture at 0.146 μ M and 1 μ M, respectively. Murine pro-B cell line Ba/F3 and human chronic myelogenous leukaemia cell line K562 were provided by the American Type Culture Collection (ATCC; Ref. CRL-12015 and CCL-243, respectively). These cell lines were tested for mycoplasma contamination every 3 months using Venor Gem Advance Pre-aliquoted Mycoplasma Detection Kit (Minerva biolabs).

Cell culture and proliferation assays. CD34 $^{+}$ cells from patients in CP-CML at diagnosis or umbilical cord blood were immunoselected (CD34 microBead Kit, Miltenyi Biotec) according to the manufacturer's instructions. Enrichment for CD34 $^{+}$ cells was ascertained by flow cytometry using an anti-CD34 monoclonal antibody (clone 581; BD Pharmingen). Ph1 $^{+}$ -CD34 $^{+}$ cells were cultured in serum free medium (SFM) StemSpan (StemCell Technologies) without growth factors.

Colony forming cell (CFC) and long term culture-initiating cell (LTC-IC) assays. For CFC assays, CD34 $^{+}$ cells were suspended (1×10^4) in 3 ml of alpha-MEM based methylcellulose medium (GF H4434, StemCell Technologies). Cells were scored and collected after 14 days incubation at 37 $^{\circ}$ C and 5% CO $_2$. After scoring, colonies were washed with PBS and kept frozen in RNAlater (Invitrogen) for subsequent analysis. LTC-IC with limiting dilution assays (LDA) were performed in StemSpan SFM (Stemcell technologies) on irradiated MS5 monolayers at several dilutions of CD34 $^{+}$ cells (300, 150, 75, or 37 cells per well for Ph1 $^{+}$ CD34 $^{+}$ cells and 200, 100, 50, or 25 cells per well for CD34 $^{+}$ from healthy donors) in 96-well plates with 16 replicate wells per concentration. After five weeks with weekly change of one half medium volume, all cells were transferred in alpha-MEM based methylcellulose medium (GF H4434, Stemcell technologies) to determine the total clonogenic cell content of each LTC. LTC-IC frequencies were determined using the L-Calc software (Stemcell technologies).

Flow cytometry. The following antibodies were used: fluorescein isothiocyanate (FITC)-conjugated IgG1 (clone 679.1M c_7 , Beckman Coulter), Alexa Fluor 488-conjugated-IgG1 (clone MOPC-21, BD Pharmingen), allophycocyanin (APC)-IgG1 (clone MOPC-21, BD Pharmingen), peridinin chlorophyll protein-cyanin 5.5 (PerCP-Cy5.5)-conjugated IgG1 (clone X40, BD Pharmingen), phycoerythrin cyanin (PE-Cy7)-conjugated IgG1 (clone MOPC-21, BD Pharmingen), (PerCP-Cy5.5)-conjugate CD45 (clone 2D1, BD Pharmingen), (APC)-conjugated CD34 (clone 581, BD Pharmingen), (PE-Cy7)-conjugated CD38 (clone HB7, BD Pharmingen), Alexa Fluor 488-conjugated anti-STAT5 (pY694) (clone 47, BD Pharmingen), (PE)-conjugated anti-GLUT1 (FAB1418P, R&D systems). For all experiments, cell viability was assessed using SYTOX Blue dead cell stain (Invitrogen Life Technologies).

Intracellular STAT5 phosphorylation assays. In brief, 3×10^5 K562 cells per ml cultured in complete Dulbecco's modified Eagle medium supplemented with 10% fetal calf serum (PAA) alone and with or without pioglitazone (10 μ M) or imatinib (1 μ M) at 37 $^{\circ}$ C in 5% CO $_2$ were harvested at variable time as indicated. Cells were fixed and permeabilized using Cytotfix/Cytoperm kit (BD Pharmingen) and stained with Alexa Fluor 488-anti-phospho-STAT5 monoclonal antibody (BD Phosflow) or Alexa Fluor 488-isotype-matched control to obtain fluorescence minus comparative in each experiment. Analysis was carried on a minimal number of 50,000 events in the viable cell gate. The delta mean fluorescence intensity of p-STAT5 after drug treatment (p-STAT5AMFI) was determined as follow: (untreated cells p-STAT5 MFI - non-treated cells isotype-control MFI) - (drug treated cells p-STAT5 MFI - drug treated cells isotype-control MFI).

CFSE assays. Fresh CD34 $^{+}$ -enriched cells were stained with 2 μ M of 5- (and 6-) carboxyfluorescein diacetate succinimidyl diester (CFSE, Invitrogen). Cells were then cultured (seeded 5.10^5 per ml) in SFM StemSpan (StemCell Technologies) without growth factors and with or without pioglitazone (10 μ M) or imatinib (1 μ M). Cells cultured in the presence of Colcemid (100 ng ml $^{-1}$, Invitrogen Life Technologies) were used to establish the range of fluorescence exhibited by cells that had not divided during post-labelling incubation. Cells were harvested at variable time points as indicated, collected in BD Truocount tubes for absolute count (BD Biosciences) and labelled with anti-CD45 and anti-CD34. Then, cells were diluted in 1 ml of phosphate-buffered saline (PBS, Invitrogen Life Technologies) containing 2% fetal calf serum (PAA) and stained for viability. All analyses were carried out on a BD FACS Canto2 Flow Cytometer.

DNA synthesis assay. Cell proliferation rate was measured by incorporation of 5-ethynyl-2'-deoxyuridine (EdU), a thymidine nucleoside analogue, in DNA during active DNA synthesis (two hours). Staining was performed according to the manufacturer's protocol (Click-iT EdU Flow Cytometry Assay Kit, Invitrogen). All analyses were carried out on a BD FACS Canto2 Flow Cytometer.

RNA extraction and RT-qPCR analysis. RNA was extracted from 2×10^5 cells using RNeasy lysis buffer (Qiagen). Reverse transcription was carried out for 1 h at 42 $^{\circ}$ C using SuperScript Vilo cDNA Synthesis kit (Invitrogen Life Technologies) according to the manufacturer's instructions. Real-time PCR was performed in an iCycler thermocycler (CFX, Bio-Rad). The primers and probes sequences for *GAPDH*, *STAT5B*, *STAT5A*, *BCR-ABL*, *ABL*, *HIF1 α* , *CITED2*, *OCT1*²⁰, *MDR1*²⁶, *SIRT1*²⁷, *STAT3*²⁸, *ALOX5*²⁹, *GLUT1*³⁰, β -catenin³¹, *PML*³², *HIF2 α* ¹⁷, *Bcl-X $_L$* , *Bcl-2*, *PIM-1*, *CIS*¹⁹, *BMI1*²², *HES-1*²³, *p57 (CDKN1C)*²³, *CD36*²¹ (known to be upregulated by PPAR γ agonists, was used as a positive control) are reported in Supplementary Table 1. The primer pairs used with TaqMan Gene Expression Master mix (Applied Biosystems) and iQ Supermix SYBR GRN (Bio-Rad) are listed in Supplementary Table 1a and Supplementary Table 1b, respectively. The comparative C $_T$ method ($\Delta\Delta C_T$) was used to compare gene expression levels between the different culture conditions (relative to *GAPDH*).

BCR-ABL/ABL quantification. qPCR experiments were performed on cDNA using the 7000 Sequence Detection System (Applied Biosystems). The *BCR-ABL/ABL* ratio was determined using FusionQuant standards (Ipsogen) according to the Europe Against Cancer protocol³³. CMR is defined as undetectable minimal residual disease (negative *BCR-ABL* transcripts) while showing a sensitivity level of at least 40,000 amplified copies of the *ABL* control gene, that is to say more than 4.5 log reduction by standardized International Scale (IS) RT-qPCR (that is, *BCR-ABL/ABL*^{IS} mRNA ratio < 0.0025%); relapse from CMR is to be declared when at least 2 consecutive positives occur 6 months apart. These criteria are consistent with the level of sensitivity routinely applied within laboratories participating in the French GBMHM Network (Group of Molecular Biologists for Hematological Malignancies).

Interphase FISH probe assay. Fluorescent *in situ* hybridization (FISH) was performed on interphase nuclei, following standard procedures and using specific probe for the t(9;22) (MetaSystems, Germany). The probe is designed as a dual-fusion assay. The red labelled probe detects an extended region at the *ABL1* locus on 9q34 and a green labelled probe hybridizes specifically to regions at the *BCR* gene on 22q11. Preparations were counterstained with 4,6-diamidino-phenylindole (DAPI) and a minimum of 50 interphase nuclei were examined. Results were recorded using a fluorescence microscope (Nikon) fitted with appropriate filters, and digital-imaging software Lucky (CaryoSystems, France).

Western blot analysis. For STAT5 protein analysis, K562 cells (2.5×10^5) were lysed in RIPA lysis buffer on ice. Whole-cell extracts were boiled for 5 min in Laemmli sample buffer and subjected to SDS-PAGE in 4–12% acrylamide gels (Nupage, Invitrogen Life Technologies). Proteins were transferred to Hybond N+ filters (Amersham). Membranes were probed with the following antibodies: STAT5 (sc-1656), ACTIN (sc-8432), PPAR γ (H-100:sc-7196), goat anti-mouse IgG-HRP (sc-2005) (Santa Cruz Biotechnology Inc.) and Anti-HIF2 α (SMC-185C/D). Antibody binding was detected by the enhanced chemiluminescence ECL+ (Amersham).

Lentiviral vector production and transduction. *STAT5B* lentiviral vector. The cDNA encoding STAT5B was cloned, sequenced (GenBank accession number DQ267926), and inserted into the SIN-cPPT-PGK-WHV lentiviral transfer vector as previously described³⁴. A SIN-cPPT-PGK-eGFP-WHV lentiviral vector was used for control.

OCT-1 and HIF2 α lentiviral vectors. OCT-1 (SLC22A1, accession number BC126364) and HIF2 α (EPAS1, accession number BC051338) lentiviral vectors were provided by Applied Biological Materials, Inc. (catalogue nos LV309003 and LV149063).

Constitutively active murine Stat5a and Stat5a. Stat5a(1*6)(H299R, S711F) and Stat5b(1*6)(H299R, S711F) retroviral vectors were provided by Cell Biolabs, Inc. (catalogue nos RTV-333 and RTV-335).

shRNA lentiviral vector anti-PPAR- γ . The PPAR- γ mRNA pairing sequence 5'-TGTTCCGTGACAATCTGTC-3' (GenBank accession number L40904) was designed and synthesized as follows within an shRNA structure comprising unique restriction sites at each end: sense 5'-GATCTCCTGTTCCGTGACAATCTGTCCTCAAGAGAACAGATTGTCACGGAAACATTTTGGAGAAGATTCC-3'; antisense 5'-CTGAGGAATCTCTCCAAAAAATGTTCCGTGACAATCTGTAAGTTCTCTACAGATTGTCACGGAAACAGGA-3'. Oligonucleotides were annealed and ligated into BglIII and XhoI sites of linearized pSuper plasmid. PolIII H1 promoter-shRNA PPAR- γ was then subcloned in the pTRIP lentiviral vector. Vectors were produced as previously described³⁴.

BCR-ABL lentiviral vector. Total RNA from K562 cells was extracted using TRIzol (Invitrogen Life Technologies). Reverse transcription was carried out for 1 h at 50 $^{\circ}$ C using SuperScript III (Invitrogen Life Technologies). Two independent PCR were performed using *BCR-ABL* F1, 5'-ATGGTGGACCCGGTGGGCTT-3' with *BCR-ABL* R 2831, 5'-CTGCTACCTCTGCACTATGTCACTG-3' and *BCR-ABL* F 2685, 5'-TCCGCTGACCATCAATAAGGA-3' with *BCR-ABL* R 6097, 5'-CTGCTACCTCTGCACTATGTCACTG-3' respectively. Specific amplification

bands were pooled, heated to 95 °C during 3 min and ramp cooled to 25 °C over a period of 45 min. Annealing product was submitted to a third PCR with *LA Taq* DNA polymerase (Takara) using the following primer pair: *BCR-ABL F 1 asc1*: 5'-AGGCGCGCCATGGTGGACCCGGTGGGCTT-3' and *BCR-ABL R 6097 sbf1*: 5'-CCTGCAGGCTGTACCTCTGCACTATGTCACTG-3'. Amplification product was subcloned into a pCR-XL-TOPO plasmid (Invitrogen Life Technologies) before being inserted into the SIV GAE-SSFV lentiviral transfer vector, followed by DNA sequencing. An SIV GAE-SSFV-eGFP vector was used as a control. The SIV vectors were produced as previously described³⁴.

CD34⁺ cell transduction. Cells were suspended ($1 \times 10^6 \text{ ml}^{-1}$) in StemSpan (StemCell Technologies, France) supplemented with protamine sulphate ($4 \mu\text{g ml}^{-1}$), SCF (100 ng ml^{-1}), FLT-3-L (100 ng ml^{-1}), IL-3 (20 ng ml^{-1}), and IL-6 (20 ng ml^{-1}), in a 96-well plate coated with RetroNectin (Takara Shuzo Co., Japan). Cell suspensions were incubated for 16 h. Lentiviral vectors were then added and cell suspensions incubated for 12 h. Cells were washed twice before being seeded.

siRNA assays. siRNA targeting the human *PPAR γ* sequence 5'-TGTTCCGTGACAATCTGTC-3' were synthesized (Sigma-Aldrich Proligo). siRNAs targeting the human *STAT5* sequence 5'-AAACTCAGGACCCTTGC-3', human *HIF2 α* sequence 5'-ATTAGAGCAAAGAGTCAGC-3' and murine *Cited2* sequence 5'-CGAGGAAGTGCTTATGTCCTT-3' were synthesized (eurofins MWG/operon). CD34⁺ BM cells were transfected with specific siRNA (25 nM) in the presence of Lipofectamine 2000 (Invitrogen) and maintained for 48 h before CFC assay. Control siRNA was purchased from Invitrogen Life Technologies (BLOCK-iT). Transfection efficiency was assessed using a fluorescein-labelled, double-strand RNA duplex (BLOCK-iT FluorescentOligo; Invitrogen).

Human patients. Fresh bone marrow from patients with chronic-phase CML at diagnosis, umbilical cord blood cells from healthy donors, and blood or bone marrow samples from diabetes patients and patient given pioglitazone off-label were obtained with informed consent approved by the hospital's Institutional Review Board (Comité de protection des personnes Ile-de-France XI) under approved protocol EudraCT number: 2009-011675-79. Imatinib levels were measured in patients' plasma using a previously described high-performance liquid chromatography (HPLC) method³⁵.

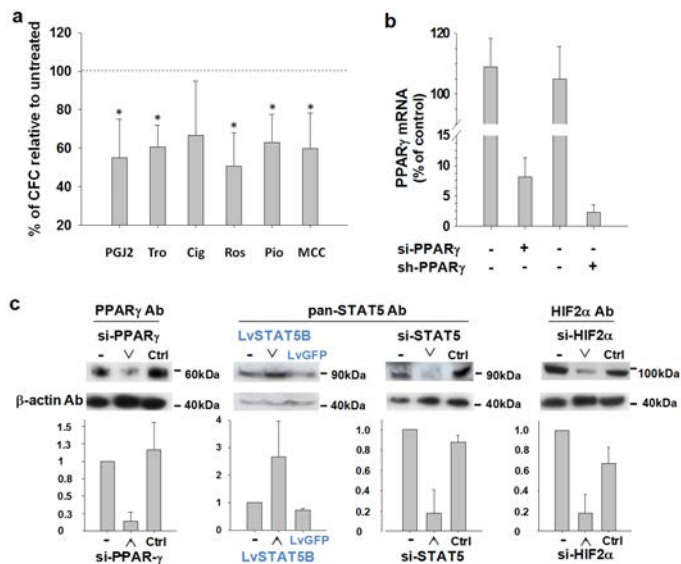
Statistical analysis. No statistical methods were used to predetermine sample size, the experiments were not randomized and the investigators were not blinded to allocation during experiments and outcome assessment. For culture assays and quantitative real-time PCR, values were calculated as mean \pm standard deviation for at least three separate experiments performed in triplicate. Paired and unpaired comparisons were made, using the nonparametric Wilcoxon rank test and the Mann-Whitney test, respectively. Limiting dilution analysis was carried out with L-Calc software (StemCell Technologies). All statistical analyses were carried out with StatView software (SAS Institute Inc., Cary, NC).

Statistical information on samples described in figures. For all culture assays, paired and unpaired comparisons were made using the nonparametric Wilcoxon rank test and the Mann-Whitney test, respectively. Fig. 1a, b, plotted are means for CD34⁺ cells from 4 CP-CML patients, 16 replica for each. Data with imatinib alone are not statistically different from those for the untreated control ($P = 0.067$), whereas pioglitazone as a single agent reduced LTC-IC frequencies by 2.4-fold ($P = 0.008$) or by 3.5-fold in combination with imatinib ($P < 0.001$). LTC-IC frequencies were established using L-Calc software (StemCell Technologies). Fig. 1c-e, All patients and statistical analysis are presented in Extended Data Table 1 ($n = 6$). Fig. 2a, *STAT5B* RT-qPCR normalized to *GAPDH* mRNA. Shown are means with standard deviations (s.d.) for 5 CP-CML patients. *STAT5B* mRNA levels decreased by 8.5-fold ($P < 0.0001$), 1.5-fold ($P = 0.08$) and 10.5-fold ($P < 0.0001$) in the presence of pioglitazone, imatinib and the drug combination, respectively. Fig. 2b, Compared to imatinib alone, RT-qPCR analysis shows that addition of pioglitazone induces a significant reduction in mRNA levels by 3.3 and 4.8 fold for *BCL-x₁* and *BCL-2*, respectively, and 1.6 fold for *PIM1* and *CIS*. mRNA

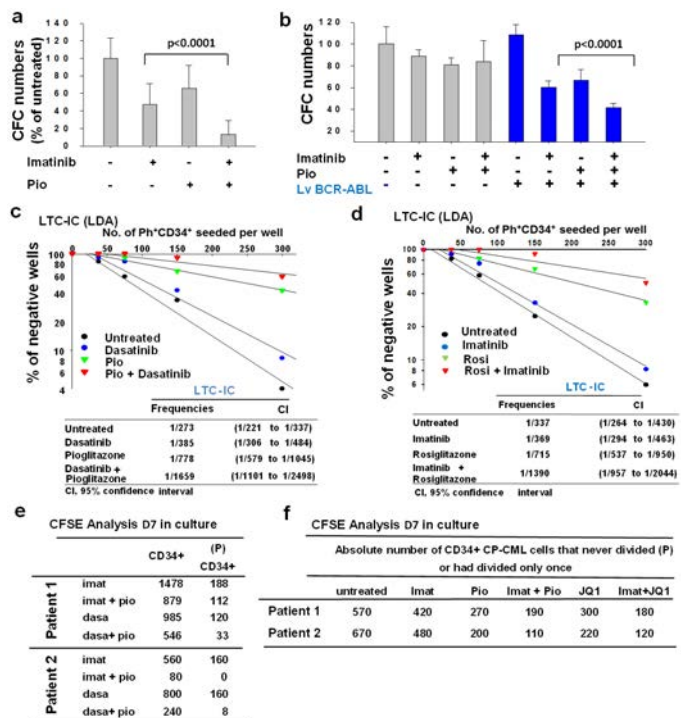
quantification are normalized to *GAPDH* levels ($n = 5$ CP-CML patients, $*P < 0.05$). Fig. 2c, Means with s.d. for 5 CP-CML patients. The effect of pioglitazone was negated by an siRNA against *PPAR γ* ($P = 0.043$); siRNA validated in Extended Data Fig. 1c. Fig. 2d, Means with s.d. for 5 CP-CML patients. *STAT5* overexpression counteract pioglitazone effect ($P = 0.0047$); Lv*STAT5* validated in Extended Data Fig. 1c. Fig. 3a, results are normalized to *GAPDH* mRNA levels and represented relative to mRNA expression for the "Imatinib alone" condition (means of 11 patients with s.d. for each mRNA assessed). Fig. 3b, results are normalized to *GAPDH* mRNA levels and represented relative to mRNA expression of "untreated cells" (means of 6 patients with s.d.). As compared to untreated controls, cells treated with imatinib alone show a 6.2-fold increase of *HIF2 α* relative to control ($P < 0.011$) and a 4.5-fold increase of *CITED2* ($P = 0.0277$). The addition of pioglitazone reduced the imatinib-mediated *HIF2 α* increase to 2.8-fold ($P = 0.027$). Pioglitazone significantly reduced *HIF2 α* induction by 2.2-fold ($P = 0.027$) and fully counteracted *CITED2* induction. Pioglitazone alone has no effect compared to control. Fig. 4b, According to IS, relapse was declared 2 consecutive positives, 6 months apart. For Extended Data Figures, statistical information is included in their legends.

Statistical information regarding synergy determination. The putative synergistic effect of multiple drugs was determined by the algorithm and definitions of the Chou-Talalay medium-effect method³⁶. The imatinib concentration required for 50% inhibition of the number of colonies obtained after CFC assay, $\text{IC}_{50}^{\text{imatinib}}$, was first determined in CD34⁺ cells from 5 CP-CML patients at diagnosis. There was marked variability between patients ($0.6 \mu\text{M} < \text{IC}_{50} < 2 \mu\text{M}$ with a median at $1 \mu\text{M}$). Accordingly, at $1 \mu\text{M}$ imatinib concentration, the percentage inhibition was $47.1\% \pm 24$ of untreated CFC numbers in our full cohort of 29 CP-CML patients (Extended Data Figure 1). Percentages of inhibition were $65.7\% \pm 26$ and $12\% \pm 15$ of untreated CFC numbers for pioglitazone alone ($10 \mu\text{M}$) and combination (imatinib $1 \mu\text{M}$, pioglitazone $10 \mu\text{M}$), respectively. A combination index (CI) < 1 defined synergy. We calculated IC_{50} and CI values with the Calcsyn software (Biosoft, Cambridge, UK). Imatinib and pioglitazone were assumed as having independent modes of action. In these conditions, CI were always less than 0.248, thus indicating synergy between the two drugs.

26. Davies, G. F., Juurink, B. H. & Harkness, T. A. Troglitazone reverses the multiple drug resistance phenotype in cancer cells. *Drug Des. Devel. Ther.* **3**, 79–88 (2009).
27. Yuan, H. et al. Activation of stress response gene *SIRT1* by BCR-ABL promotes leukemogenesis. *Blood* **119**, 1904–1914 (2012).
28. Pitulis, N., Papageorgiou, E., Tenta, R., Lembessis, P. & Koutsilieris, M. IL-6 and *PPAR γ* signalling in human PC-3 prostate cancer cells. *Anticancer Res.* **29**, 2331–2337 (2009).
29. Chen, Y., Hu, Y., Zhang, H., Peng, C. & Li, S. Loss of the *Alox5* gene impairs leukemia stem cells and prevents chronic myeloid leukemia. *Nature Genet.* **41**, 783–792 (2009).
30. Korninsky, D. J. et al. Abnormalities in glucose uptake and metabolism in imatinib-resistant human BCR-ABL-positive cells. *Clin. Canc. Res.* **15**, 3442–3450 (2009).
31. Lu, D. & Carson, D. A. Repression of beta-catenin signaling by *PPAR* gamma ligands. *Eur. J. Pharmacol.* **636**, 198–202 (2010).
32. Ito, K. et al. A PML-PPAR- δ pathway for fatty acid oxidation regulates hematopoietic stem cell maintenance. *Nature Med.* **18**, 1350–1358 (2012).
33. Gabert, J. et al. Standardization and quality control studies of 'real-time' quantitative reverse transcriptase polymerase chain reaction of fusion gene transcripts for residual disease detection in leukemia — a Europe Against Cancer program. *Leukemia* **17**, 2318–2357 (2003).
34. Nègre, D. et al. Characterization of novel safe lentiviral vectors derived from simian immunodeficiency virus (SIVmac251) that efficiently transduce mature human dendritic cells. *Gene Ther.* **7**, 1613–1623 (2000).
35. Roth, O. et al. Imatinib assay by HPLC with photodiode-array UV detection in plasma from patients with chronic myeloid leukemia: comparison with LC-MS/MS. *Clin. Chim. Acta.* **411**, 140–146 (2010).
36. Chou, T. C. Drug combination studies and their synergy quantification using the Chou-Talalay method. *Cancer Res.* **70**, 440–446 (2010).

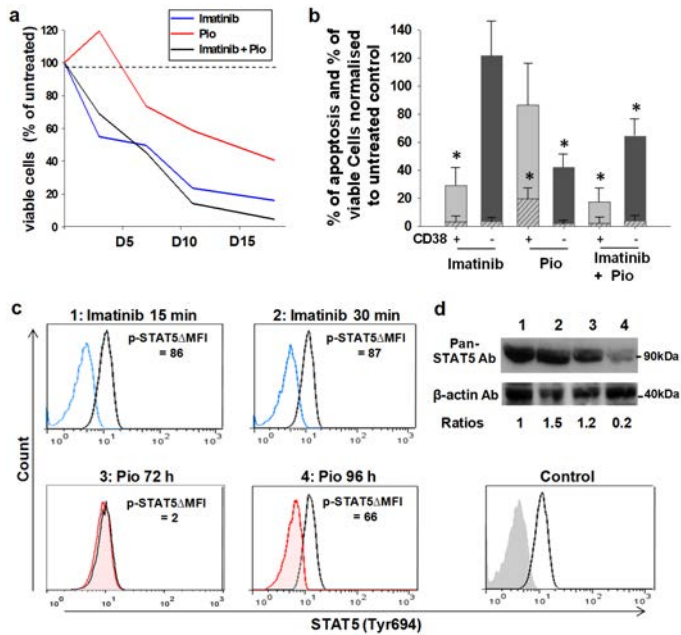


Extended Data Figure 1 | Clonogenic assays in the presence of various PPAR γ agonists and validation of STAT5B overexpression and anti-PPAR γ , anti-STAT5 and anti-HIF2 α siRNA. **a**, Clonogenic capacities of BM CD34⁺ cells were assayed following pre-incubation for 2 days with culture medium alone (control) or supplemented with PPAR γ agonists, PGJ₂, troglitazone (Tro), ciglitazone (Cig), rosiglitazone (Ros), pioglitazone (Pio) or MCC-555 (MCC) (25 μ M each) (samples from 4 donors in triplicate). The number of colonies scored is expressed as percentage of control (untreated) values with standard deviation (s.d.), * $P < 0.05$ using the nonparametric Wilcoxon rank test. **b**, Validation of anti-PPAR γ siRNA used in Fig. 2b. CD34⁺ cells were transfected with irrelevant or PPAR γ targeting siRNA (25 nM each). An anti-PPAR γ shRNA was used as a positive control. PPAR γ transcripts were normalized to GAPDH transcripts and expressed relative to the levels measured in untransfected cells. **c**, Western blot analysis with PPAR γ , pan-STAT5, HIF2 α and anti-actin antibodies (Ab). Validation of siRNA against PPAR γ or STAT5 and lentivector expressing STAT5B (LvSTAT5B) were realized on CD34⁺ cells from human UCB. Validation of siRNA against HIF2 α was realized on K562 cell line. Ctrl, scrambled siRNA; -, untreated. Quantification of western blot signal was realized with ImageJ software (<http://rsb.info.nih.gov/ij/>). Histograms show mean values with s.d., $n = 3$.

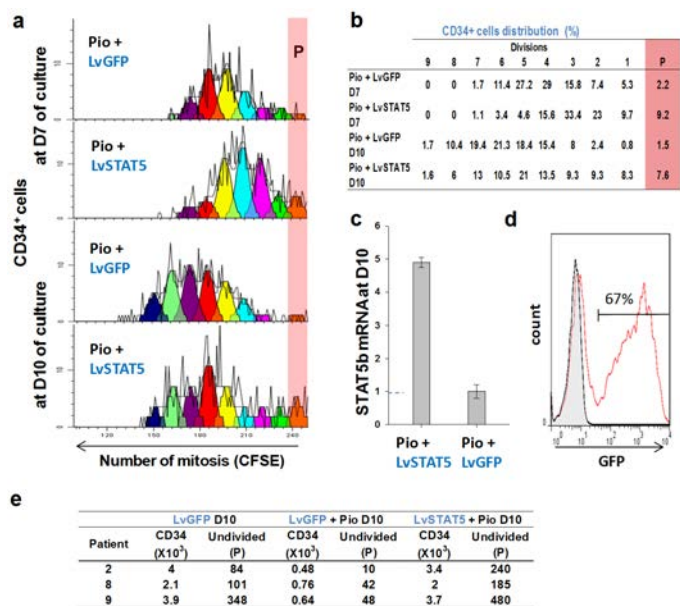


Extended Data Figure 2 | Differential and synergistic effects of pioglitazone and TKIs on CML cells.

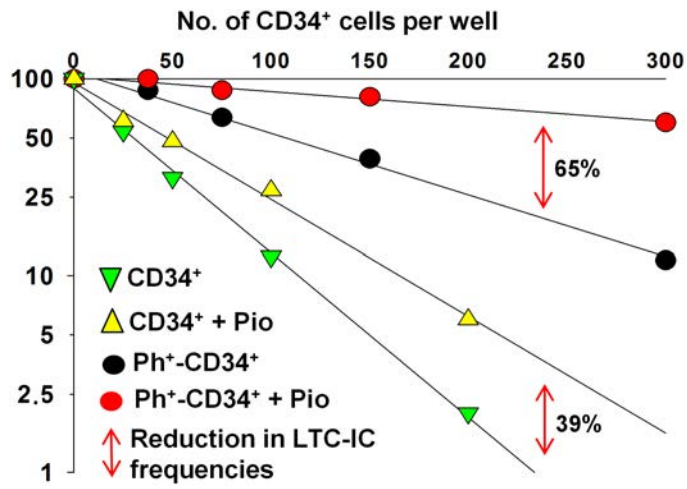
a, CFC assays with CD34⁺ CP-CML cells from patients at diagnosis. Imatinib and/or pioglitazone were added for 48h before CFC assays. Means of 29 patients with standard deviation (s.d.). **b**, CFC assays after lentivector-mediated expression of BCR-ABL or eGFP (negative control) in human cord blood CD34⁺ cells. Imatinib and/or pioglitazone were added for 48 h before CFC assays. Means of 3 individuals in triplicate with s.d. **c, d**, Limited dilution analysis (LDA) of CML LSCs by LTC-IC and frequency analysis. Plotted are means for CD34⁺ cells from 2 CP-CML patients, 16 replica each. Imatinib 1 μ M, Rosi 10 μ M. **e, f**, CFSE analysis of CD34⁺ cells (>96% Ph⁺) from CP-CML patients (for all experiments, imatinib 1 μ M, dasatinib 0.146 μ M, pioglitazone and rosiglitazone 10 μ M, JQ1 1 μ M. imat, imatinib; dasa, dasatinib; pio, pioglitazone; (P), undivided). To confirm the pivotal role played by STAT5 in the mechanism of action of pioglitazone in eroding the pool of TKI-resistant CML-LSCs, we investigated here the effect of the bromodomain inhibitor JQ1, which inhibits the transcriptional function of STAT5 by decreasing its activity through targeting the bromodomain-containing protein 2 (BRD2), a key cofactor of STAT5. Although this study with JQ1 is corroborative, one cannot completely exclude the possibility that these effects are coincidental, as targeting BRDs may cause a series of effects independent of STAT5.



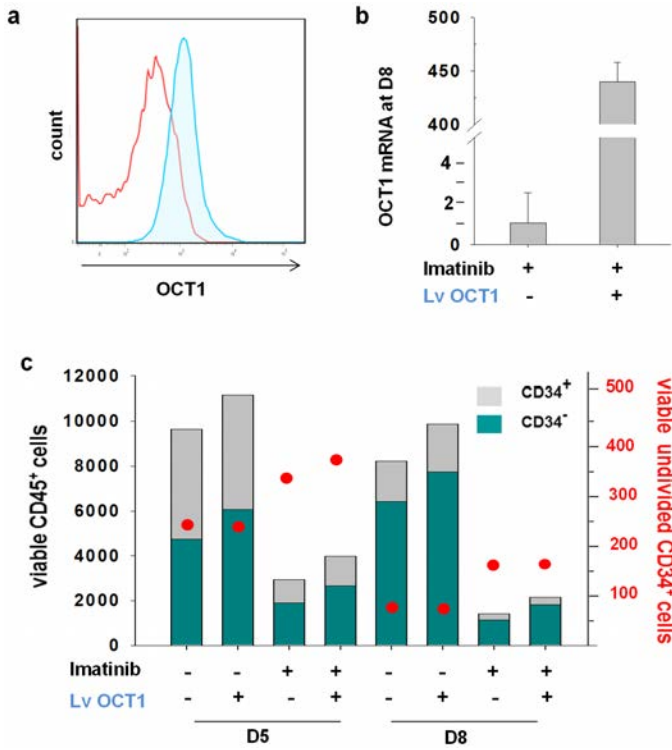
Extended Data Figure 3 | Pioglitazone slowly decreases STAT5 expression whereas imatinib rapidly inhibits STAT5 phosphorylation. **a**, Differential kinetics of action of imatinib and pioglitazone. CD34⁺ CP-CML cells (patient 4) in liquid culture in serum-free medium without cytokines. **b**, Rate of apoptosis in CP-CML cell populations after 4 days of culture with imatinib and/or pioglitazone ($n = 5$; $*P < 0.05$). Solid bars (black for CD38⁻ and grey for CD38⁺), percentage of recovery relative to input and normalized to untreated controls. Hatched bars, percentage of apoptosis, defined by the expression of annexin V. **c**, Flow cytometry analysis of permeabilized K562 cells with IgG against phosphorylated (Tyr694) STAT5. Untreated (black) and drug treated (red or blue). Control panel, no drug treatment but irrelevant IgG isotype control (grey peak). **d**, Western blot analysis with pan-STAT5 and anti-actin antibodies, showing a decrease of STAT5 by 3.5 fold \pm 0.5 (s.d.) in lane 4 ($n = 3$). Lanes 1 and 2 for imatinib (15 and 30 min exposure, respectively); lanes 3 and 4 for Pio (72 and 96 h exposure, respectively). Ratio indicates ratio of STAT5 expression/ β -actin expression relative to lane 1. Quantification of western blot signals ($n = 3$ for each condition) was realized with ImageJ software (<http://rsb.info.nih.gov/ij/>).



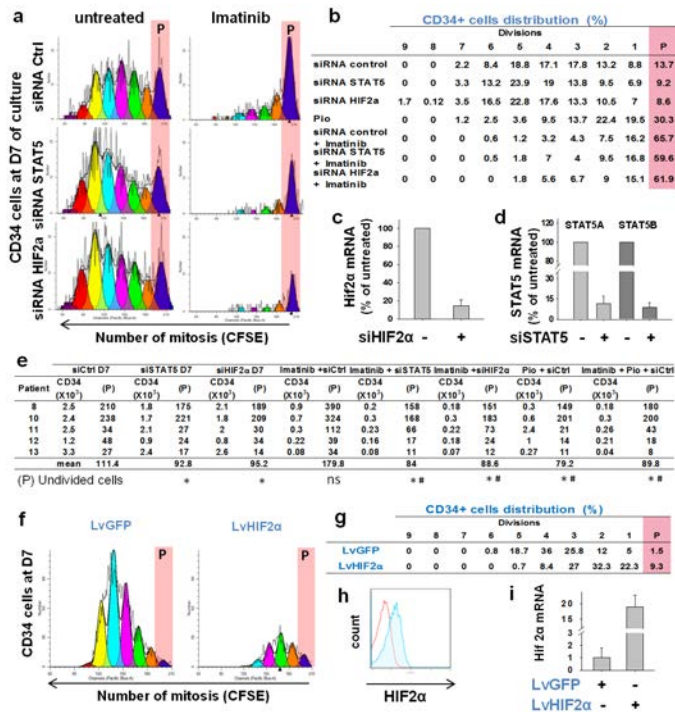
Extended Data Figure 4 | Forced expression of STAT5 in CP-CML CD34⁺ cells increases the compartment of quiescent cells. **a**, CFSE analysis of CP-CML CD34⁺ cells treated with pioglitazone after transduction with lentivectors (Lv) expressing eGFP or STAT5B, whose transcription is PPAR γ -independent. Representative CP-CML patient 2 in triplicate (data for all patients are in Extended Data Fig. 2e). One coloured peak for each cell division number. P, colcemid arrested “parent-cells”. **b**, Distribution (%) of CD34⁺ cells in each division peak shown in Extended Data Fig. 3a. **c**, *STAT5* mRNA expression analysis. **d**, Transduction efficiency of STAT5 lentivector. (5 replica with s.d.). **e**, Data for the 3 patients tested.



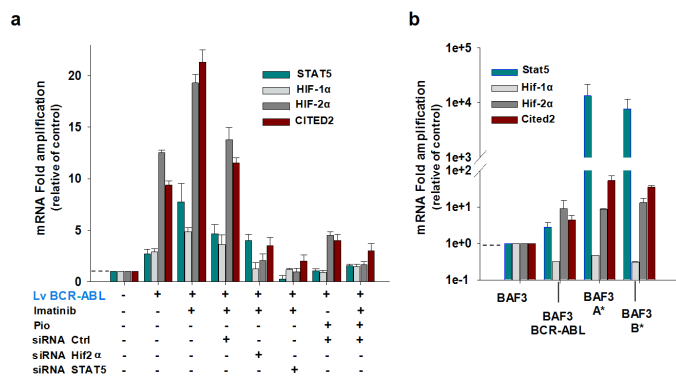
Extended Data Figure 5 | High toxicity of pioglitazone for CML LSCs vs. low toxicity for normal HSCs. LTC-IC (LDA) showing differential toxicity of pioglitazone for CP-CML vs. normal CD34⁺ cells ($n = 3, 16$ replica for each).



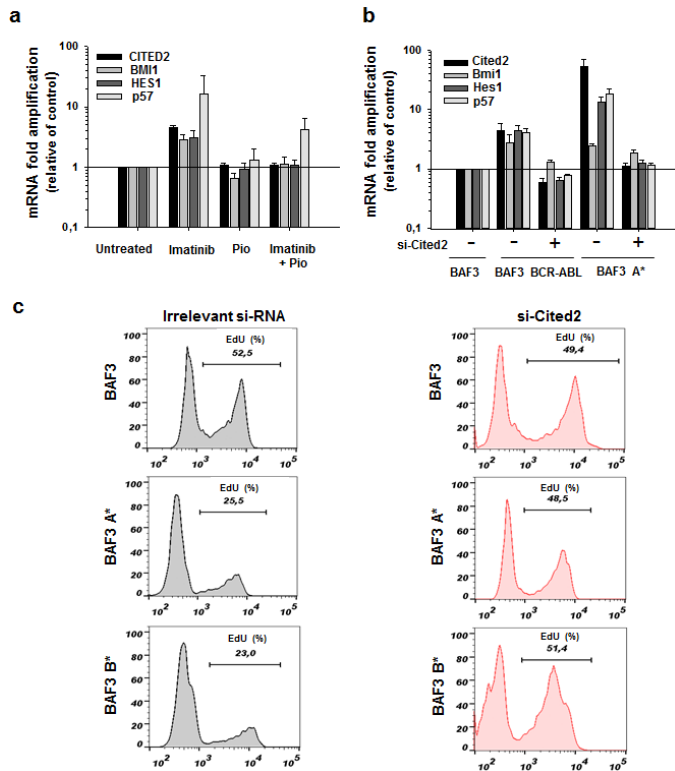
Extended Data Figure 6 | Erosion of undivided and imatinib-resistant CD34⁺ CP-CML cells is OCT1-independent. **a**, Efficiency of LvOCT1 transduction (D8). **b**, *OCT1* mRNA expression. Results are normalized to *GAPDH* mRNA levels and represented relative to mRNA expression for the “imatinib alone” condition. **c**, CFSE analysis and absolute cell count in the presence of imatinib, with or without OCT1 overexpression. Left scale (black), total cells showing CD34⁺ vs. CD34⁻ cells (histograms). Right scale (red), undivided CD34⁺ cells (red dots) (representative for $n = 3$ CP-CML patients).



Extended Data Figure 7 | The viability of undivided (P) and imatinib-resistant CD34⁺ CP-CML cells depend on HIF2α expression. Representative CP-CML patient 8 in triplicate (data for all patients are in Extended Data Fig. 6e). **a**, CFSE analysis in presence of siRNA against STAT5 or HIF2α in CD34⁺-Ph⁺ cells treated or not with imatinib. One colored peak for each cell division number. P, colchemid arrested 'parent-cells'. **b**, Distribution (%) of CD34⁺ cells in each division peak. **c**, *HIF2α* mRNA expression 72 h after siHIF2α transfection. **d**, *STAT5* A and B mRNA expression 72 h after siSTAT5 transfection into human UCB CD34⁺ cells. Results are normalized to *GAPDH* mRNA levels (means of 5 experiments with s.d. for each gene assessed). **e**, Data for the 5 patients tested (**P* < 0.05 relative to siCtrl; #*P* < 0.05 relative to Imatinib + siCtrl). **f**, CFSE analysis of cord blood CD34⁺ cells after transduction with lentivectors (Lv) expressing HIF2α or eGFP. One coloured peak for each cell division number. P, colchemid arrested 'parent-cells'. **g**, Distribution (%) of CD34⁺ cells in each division peak (*n* = 5). **h**, Transduction efficiency of HIF2α Lv. **i**, *HIF2α* mRNA expression (means of 5 experiments with s.d.).



Extended Data Figure 8 | Expression of target genes in CD34⁺ cells and Ba/F3 cell line CML-models. **a**, mRNA expression of target genes in CD34⁺ cells from UCB transduced or not by BCR-ABL expressing lentivector (Lv). BCR-ABL⁺ cells were cultured in serum-free medium without cytokines for 7 days with either imatinib alone (1 μM) or imatinib and pioglitazone (1 μM and 10 μM, respectively) (means of 5 experiments with s.d. for each gene assessed). Results are normalized to *GAPDH* mRNA levels and represented relative to mRNA expression for the 'untreated' condition. Overexpression of BCR-ABL in CD34⁺ cells from umbilical cord blood induced expression of *STAT5* and *HIF1α* mRNAs by 2.7- and 2.8-fold, respectively ($P = 0.043$), while *HIF2α* and *CITED2* mRNAs were increased by 12.5-fold and 9-fold ($P = 0.043$), respectively. In the presence of imatinib, *STAT5* and *HIF1α* mRNAs were increased by 7.5- and 4.9-fold ($P = 0.043$), respectively, while *HIF2α* and *CITED2* were increased by 19.3- and 22-fold ($P = 0.043$), respectively. Either pioglitazone or an siRNA against *STAT5* (A and B) significantly reduced the levels of *HIF2α* and *CITED2* mRNAs, while an siRNA against *HIF2α* significantly reduced *CITED2* mRNA expression (>threefold each, $P < 0.05$). **b**, mRNA expression of target genes in Ba/F3 cell sub-lines independent of IL3 for viability after transduction with LvBCR-ABL or constitutively activated Stat5A1*6 (A*) or Stat5B1*6 (B*). Results are normalized to *GAPDH* mRNA levels and represented relative to mRNA expression for the original Ba/F3 cell line (means of 5 experiments with s.d. for each gene assessed). Forced expression of *BCR-ABL* increased the level of murine endogenous *Stat5* (a and b) mRNAs by 2.7 fold ($P = 0.043$). When *BCR-ABL* or constitutively activated murine *Stat5* 1*6 (a or b) were overexpressed, murine endogenous *Hif1α* mRNA level was decreased by threefold ($P = 0.043$) and murine endogenous *Hif-2α* and *Cited2* mRNAs increased by more than eightfold each ($P = 0.043$).



Extended Data Figure 9 | The key regulator of HSC quiescence, *CITED2*, is overexpressed in TKI-resistant CD34⁺ cells from CP-CML patients.

a, mRNA expression of *CITED2* and target genes thereof *BMI1*, *HES1* and *p57* after 9 days of culture with or without imatinib and pioglitazone. Results are normalized to GAPDH ($n = 4$). **b**, mRNA expression of endogenous murine *Cited2* and its target genes *Bmi1*, *Hes1* and *p57* in Ba/F3 cell line with or without forced expression of BCR-ABL or constitutively active Stat5A 1*6 (A*) in the presence or not of siRNA against *Cited2*. Results are normalized to GAPDH (mean \pm s.d. of 3 independent experiments in triplicate). Forced expression of a constitutively active form of murine Stat5 1*6 (A or B) in Ba/F3 cells, in and of itself, was sufficient to increase endogenous expression of murine *Cited2* markedly (52-fold) as well as that of its target genes *Bmi1* (2.5-fold), *Hes1* (13-fold) and *p57* (18-fold) **c**, Proliferation analysis by EdU incorporation assay of the Ba/F3 cell line that expresses or not constitutively active forms of Stat5 A 1*6 (A*) or B 1*6 (B*) in the presence or not of siRNA against *Cited2* (representative result of 5 independent experiments).

Extended Data Table 1 | CFSE analysis of CD34⁺ cells (>96% Ph⁺) from 6 CP-CML patients after liquid culture without cytokines

Patient	Untreated D10		Imatinib D10		Pio D10		Imatinib + Pio D10	
	CD34 (x10 ³)	Undivided (P)	CD34 (x10 ³)	Undivided (P)	CD34 (x10 ³)	Undivided (P)	CD34 (x10 ³)	Undivided (P)
2	13	310	4.0	410	6.0	60	0.8	45
3	3.6	44	0.6	60	2.8	22	0.5	15
4	15	129	3.6	150	6.0	69	2.3	27
5	3.0	99	1.0	132	0.7	60	0.5	81
6	15	128	2.4	63	9.0	35	1.3	48
7	7.8	220	1.3	251	1.8	153	0.8	107
mean	155			177.6		66.5		53.8

